

Macroscopic equations for a binary gas mixture

Tatiana G. Elizarova*, Irina A. Graur* and Jean-Claude Lengrand†

**Institute for Mathematical Modeling*¹, *Russian Acad. of Sci., Moscow, Russia*

†*Laboratoire d'Aérodynamique du CNRS, Orléans, France*

Abstract. The derivation of moment equations for the description of a flowing binary non-reacting gas mixture is presented. The equations obtained are based on a kinetic model in a relaxation form and can be regarded as the extension of the quasigasdynamic equations (QGD) studied before. As an example of implementation the results for the shock wave structure in an argon-xenon mixture and for the binary diffusion process of argon and helium are presented in comparison with the DSMC results.

I INTRODUCTION

There are two groups of models for calculating gas-mixture flows. The first one consists of kinetic models, i.e. models based on direct numerical simulation methods (DSMC) or on the solution of the Boltzmann equation (e.g. [1]). The other group consists of systems of macroscopic equations which are derived on the basis of Navier-Stokes equations, in general by a phenomenological way (e.g. [2] – [4]).

In this paper we propose a new macroscopic model to describe flows of a binary non-reacting gas mixture. The model is a two-fluid approximation that consists of a system of equations for density, momentum and energy of each component. The system of macroscopic equations (named QGDM) is based on the kinetic equation in its relaxation approximation and is a natural generalization of the recently proposed quasigasdynamic (QGD) equations (e.g. [5] – [7]) for a gas mixture. Note that previously the QGD equations were generalized for gas flows in translational [8] and rotational [9] non-equilibrium.

II KINETIC MODEL AND MACROSCOPIC EQUATIONS

We consider a mixture consisting of gas a and gas b . Each gas is characterized by its density ρ_i , temperature T_i and macroscopic velocity \vec{u}_i , where $i = a, b$. We introduce the gas constant $R_i = k/m_i$, where k is the Boltzmann constant, m_i is the mass of the molecule. According to [10] the kinetical model for the mixture can be expressed as

$$\frac{\partial f_a}{\partial t} + (\vec{\xi} \nabla) f_a = \nu_{aa}(F_a - f_a) + \nu_{ab}(\bar{F}_a - f_a), \quad (1)$$

$$\frac{\partial f_b}{\partial t} + (\vec{\xi} \nabla) f_b = \nu_{bb}(F_b - f_b) + \nu_{ba}(\bar{F}_b - f_b), \quad (2)$$

where f_a and f_b are the distribution functions for species, $\vec{\xi}$ is the molecule velocity, ν_{aa} and ν_{bb} are the frequencies of self-collisions, ν_{ab} is the frequency of collisions of a molecules with b molecules, ν_{ba} is the frequency of collisions of b molecules with a molecules. F_a , F_b and \bar{F}_a , \bar{F}_b are Maxwellian distribution functions based on (u_a, T_a) , (u_b, T_b) , (\bar{u}_a, \bar{T}_a) , (\bar{u}_b, \bar{T}_b) . The so-called free parameters (overlined symbols) can be expressed in terms of parameters m, \vec{u}, T of each gas

¹⁾ This work was sponsored by the Russian Foundation for Basic Research, project no.98-01-00155

$$\begin{aligned}
\bar{u}_a &= \bar{u}_b = \frac{m_a \bar{u}_a + m_b \bar{u}_b}{m_a + m_b}, \\
\bar{T}_a &= T_a + \frac{2m_a m_b}{(m_a + m_b)^2} \left(T_b - T_a + \frac{m_b}{6k} (\bar{u}_b - \bar{u}_a)^2 \right), \\
\bar{T}_b &= T_b + \frac{2m_a m_b}{(m_a + m_b)^2} \left(T_a - T_b + \frac{m_a}{6k} (\bar{u}_b - \bar{u}_a)^2 \right).
\end{aligned} \tag{3}$$

We suppose that the distribution functions can be approximated by a gradient expansions as in [8]

$$f_i = F_i - \tau(\xi^{\vec{\nabla}})F_i \tag{4}$$

where τ is identified with μ/p , μ is the viscosity and p the pressure of the mixture. These expressions are substituted for f_a and f_b into the convective terms of Eqs.1-2 to yield an approximation of these equations

$$\frac{\partial f_a}{\partial t} + (\xi^{\vec{\nabla}})F_a - (\xi^{\vec{\nabla}})\tau(\xi^{\vec{\nabla}})F_a = \nu_{aa}(F_a - f_a) + \nu_{ab}(\bar{F}_a - f_a), \tag{5}$$

$$\frac{\partial f_b}{\partial t} + (\xi^{\vec{\nabla}})F_b - (\xi^{\vec{\nabla}})\tau(\xi^{\vec{\nabla}})F_b = \nu_{bb}(F_b - f_b) + \nu_{ba}(\bar{F}_b - f_b). \tag{6}$$

Equations 5 and 6 are integrated over the velocity space after multiplications by 1, $\xi^{\vec{\nabla}}$ and $\xi^{\vec{\nabla}^2}/2$, successively and result in a system (QGDM) of macroscopic equations for the binary mixture

$$\frac{\partial}{\partial t}\rho_a + \nabla_i \rho_a u_a^i - \nabla_i \tau (\nabla_j \rho_a u_a^i u_a^j + \nabla^i p_a) = 0, \tag{7}$$

$$\frac{\partial}{\partial t}\rho_a u_a^k + \nabla_i \rho_a u_a^i u_a^k + \nabla^k p_a = \nabla_i \tau (\nabla_j \rho_a u_a^i u_a^j u_a^k + \nabla^i p_a u_a^k + \nabla^k p_a u_a^i) + \nabla^k \tau \nabla_i p_a u_a^i + S_a^u, \tag{8}$$

$$\begin{aligned}
\frac{\partial}{\partial t}E_a + \nabla_i u_a^i (E_a + p_a) &= \nabla_i \tau (\nabla_j (E_a + 2p_a) u_a^i u_a^j + \frac{1}{2} \nabla^i u_{ak} u_a^k p_a) + \\
\frac{\gamma_a}{\gamma_a - 1} \nabla_i \tau \frac{p_a}{\rho_a} \nabla^i p_a + Pr_a^{-1} \frac{\gamma_a}{\gamma_a - 1} \nabla_i \tau p_a \nabla^i \frac{p_a}{\rho_a} &+ S_a^E,
\end{aligned} \tag{9}$$

where the volumic energy writes

$$E_a = (\rho_a \bar{u}_a^2)/2 + p_a/(\gamma_a - 1) \quad \text{with } p_a = \rho_a R_a T_a. \tag{10}$$

Similar equations hold for gas b . The Prandtl number Pr and specific heat ratio γ do not appear in the above-described treatment and have been introduced artificially for generalization purpose to make these equations coincide with Navier-Stokes (NS) equations in the case of a one-species gas and vanishing Knudsen numbers ($\tau \rightarrow 0$) [7].

The exchange terms S result from the integration of the right-hand sides of the equations 5, 6 and are recognized as

$$S_a^u = \nu_{ab} \rho_a (\bar{u}_a - \bar{u}_a), \quad S_b^u = \nu_{ba} \rho_b (\bar{u}_b - \bar{u}_b), \quad S_a^E = \nu_{ab} (\bar{E}_a - E_a), \quad S_b^E = \nu_{ba} (\bar{E}_b - E_b), \tag{11}$$

where \bar{E}_a and \bar{E}_b have expressions similar to E_a in Eq.10.

$$S_a^u + S_b^u = 0, \quad S_a^E + S_b^E = 0 \tag{12}$$

which is consistent with momentum and energy conservation.

Thus the binary mixture has been described by a self-contained set of two-fluid equations which allows for different velocities and temperatures of the components.

The mixture parameters (no subscript) relate to the species parameters:

$$\begin{aligned}
n &= n_a + n_b, \quad \rho = \rho_a + \rho_b, \quad p = p_a + p_b, \quad u = (\rho_a u_a + \rho_b u_b)/\rho, \\
T &= (n_a T_a + n_b T_b)/n, \quad m = (m_a n_a + m_b n_b)/n, \quad p = \rho RT, \\
R &= (\rho_a R_a + \rho_b R_b)/\rho = k/m.
\end{aligned} \tag{13}$$

III DETERMINATION OF COLLISION FREQUENCIES

To close the system of QGDM equations, it is necessary to estimate the cross-collision frequencies ν_{ab} and ν_{ba} and the relaxation time τ .

Relations between frequencies of collisions of a molecules with each other (self-collisions) and with b molecules (cross-collisions), according to [10], can be calculated in the following way:

$$\nu_{ab} = \nu_a \left(\frac{d_{ab}}{d_a} \right)^2 \sqrt{\frac{m_a + m_b}{2m_a m_b} \frac{n_a}{n_b}}, \quad (14)$$

where d_a is the effective molecular diameter for gas a , d_{ab} is the effective diameter which can be determined, for example, according to [1], p.16, as $d_{ab} = 0.5(d_a + d_b)$. In turn, the collision frequency ν_a can be related to with the gas viscosity in the approximation of the VHS and VSS models for particle interactions ([1], p.90):

$$\nu_a = \frac{p_a}{\mu_a} \Omega(\omega_a, \alpha_a), \quad \mu_a = \mu_{aref} \left(\frac{T_a}{T_{aref}} \right)^{\omega_a},$$

$$\text{where } \Omega(\omega_a, \alpha_a) = \frac{5(\alpha_a + 1)(\alpha_a + 2)}{\alpha_a(7 - 2\omega_a)(5 - 2\omega_a)}. \quad (15)$$

For further calculations $\alpha_a = 1$ is used, that conforms to the VHS model ([1], p.41). In this case we write $\Omega(\omega_a, 1) = \Omega(\omega_a)$.

The total number of collisions between molecules of gases a and b should be balanced, i.e. relation $n_a \nu_{ab} = n_b \nu_{ba}$ must be satisfied.

To estimate the relaxation time $\tau = \mu/p$ we determine the binary-mixture viscosity using the Wilke formula [3]:

$$\mu = \mu_a \left(1 + G_{ab} \frac{\rho_b \mathcal{M}_a}{\rho_a \mathcal{M}_b} \right)^{-1} + \mu_b \left(1 + G_{ba} \frac{\rho_a \mathcal{M}_b}{\rho_b \mathcal{M}_a} \right)^{-1},$$

$$\text{where } G_{ab} = \frac{\left(1 + \sqrt{\mu_a / \mu_b} \sqrt{\mathcal{M}_b / \mathcal{M}_a} \right)^2}{2\sqrt{2} (1 + \mathcal{M}_a / \mathcal{M}_b)}, \quad (16)$$

where \mathcal{M}_a and \mathcal{M}_b are the molar masses of gases a and b respectively.

Note, that the collision frequencies and the binary-mixture viscosity are parameters “external” to the QGDM model and could be determined by other estimations.

IV SHOCK WAVE STRUCTURE IN A HELIUM - XENON MIXTURE

As a first example of using the QGDM equations we considered the problem of a stationary shock wave structure in a mixture of helium (He is gas a) and xenon (Xe is gas b). Density profiles for these gases, measured with the use of an electron gun and a laser interferometer, can be found in [11]. Measurements were performed for the following variants:

- variant V1 - 98,5% He and 1.5% Xe
- variant V2 - 97% He and 3% Xe
- variant V3 - 94% He and 6% Xe
- variant V4 - 91% He and 9% Xe

For variant V2, there is a calculation by the DSMC method [1], the results of which can be considered as a reference. It coincides practically with the experimental data.

The system of equations (7) - (9) is solved in non-dimensional variables taking as dimensional scales the following characteristics of gas a in the upstream flow: ρ_{aref} is the density, $a_{aref} = \sqrt{\gamma_a R_a T_{aref}}$ is the sound velocity at temperature T_{aref} , λ_{aref} is the mean free path, that is computed as in [1]:

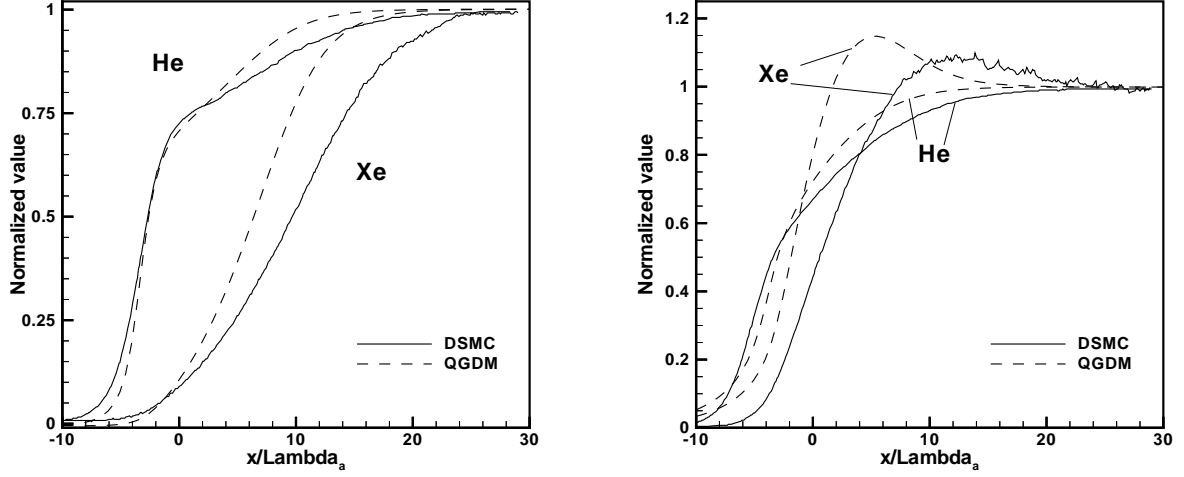


FIGURE 1. Density (a) and temperature(b) profiles in a He-Xe mixture

$$\lambda = \frac{4\mu}{\rho\sqrt{RT}} \frac{1}{\sqrt{2\pi}\Omega(\omega)}. \quad (17)$$

Then relations between the dimensional and dimensionless parameters have the following forms (all parameters of gas b are scaled by parameters of gas a):

$$\rho = \tilde{\rho}\rho_{aref}, \quad a = \tilde{a}a_{aref}, \quad u = \tilde{u}a_{aref}, \quad p = \tilde{p}\rho_{aref}a_{aref}^2, \quad m = \tilde{m}\rho_{aref}\lambda_{aref}^3,$$

$$T = \tilde{T} \frac{a_{aref}^2}{\gamma_a R_a} = \tilde{T} T_{aref}, \quad x = \tilde{x}\lambda_{aref}, \quad t = \tilde{t} \frac{\lambda_{aref}}{a_{aref}}, \quad n = \tilde{n} \frac{1}{\lambda_{aref}^3}.$$

QGDM equations do not change their forms after the process of scaling. The relations between the parameters of the gases (link equations) write as

$$\tilde{a}_a = \sqrt{\tilde{T}_a}, \quad \tilde{a}_b = \sqrt{\frac{\gamma_b R_b}{\gamma_a R_a} \tilde{T}_b}, \quad \tilde{T}_a = \frac{\gamma_a \tilde{p}_a}{\tilde{\rho}_a}, \quad \tilde{T}_b = \frac{\gamma_a \tilde{p}_b R_a}{\tilde{\rho}_b R_b},$$

$$\tilde{\mu}_a = \tilde{T}_a^{\omega_a}, \quad \tilde{\mu}_b = \frac{\mu_{bref}}{\mu_{aref}} \left(\frac{T_{aref}}{T_{bref}} \right)^{\omega_b} \tilde{T}_b^{\omega_b},$$

here μ_{bref} and T_{bref} are the viscosity coefficient and the corresponding temperature of gas b , used in the viscosity-law (15).

Table VI presents the parameters of the mixture before the shock wave, chosen in accordance with the experimental data from [11] and with the calculation from [1]. The Prandtl number for the gases is constant and equal to $Pr = 2/3$.

The boundary conditions on the right and left boundaries were taken from the Rankine-Hugoniot conditions for a stationary shock wave in a gas mixture. The variables on the right of the discontinuity are computed as follows

$$\begin{aligned} \rho_2 &= \rho_1 \frac{(\gamma + 1)Ma^2}{2 + (\gamma - 1)Ma^2}, & p_2 &= p_1 \frac{2\gamma Ma^2 - \gamma + 1}{\gamma + 1}, \\ u_2 &= u_1 \frac{2 + (\gamma - 1)Ma^2}{(\gamma + 1)Ma^2}, \end{aligned} \quad (18)$$

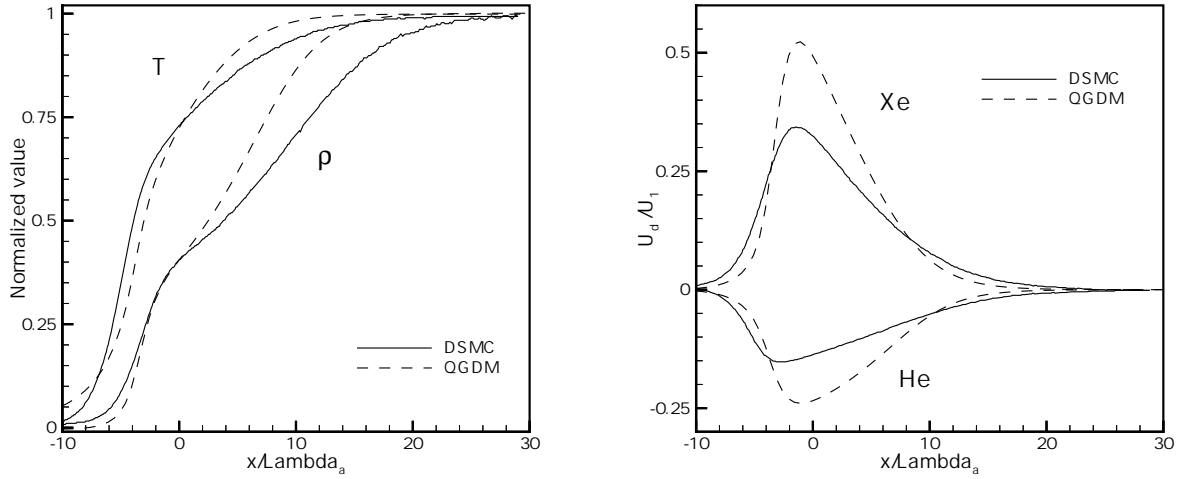


FIGURE 2. Mean temperature and density profiles (a) and diffusion velocities (b) in a He-Xe mixture

where subscripts 1 and 2 refer to Rankine-Hugoniot conditions upstream (1) and downstream (2) of the shock wave. The component temperatures are found from the equations of state.

Assume that the temperatures and velocities of the components before and after the shock wave are equal, and the mass-fraction of the components after the transition through the shock are unchanged ($n_{a1}/n_1 = n_{a2}/n_2$, $n_{b1}/n_1 = n_{b2}/n_2$). Thus on the basis of conditions (18), the parameters of each component of the mixture are derived from the ratios:

$$\begin{aligned} \rho_{a2} &= m_a n_{a2}, & T_{a1} &= T_{b1} = T_1, & u_{a1} &= u_{b1} = u_1, \\ \rho_{b2} &= m_b n_{b2}, & T_{a2} &= T_{b2} = T_2, & u_{a2} &= u_{b2} = u_2. \end{aligned} \quad (19)$$

The initial conditions are a discontinuity at point $x = 0$:

$$\begin{aligned} \text{at } x \leq 0 & \quad \rho_a = \rho_{a1}, \quad \rho_b = \rho_{b1}, \quad T_a = T_b = T_1, \quad u_a = u_b = u_1. \\ \text{at } x \geq 0 & \quad \rho_a = \rho_{a2}, \quad \rho_b = \rho_{b2}, \quad T_a = T_b = T_2, \quad u_a = u_b = u_2. \end{aligned} \quad (20)$$

To solve the (7) - (9) system, an explicit difference scheme was applied where the steady-state solution was obtained as the limit of a time-evolving process. All spatial derivatives, including the convective terms, were approximated by central differences (see, for instance, [12]).

The problem was solved using a uniform spatial grid with a convergence criterion $\epsilon_{\rho_a} = 10^{-5}$. When refining the grid by a factor of 2, the differences between the computational results were extremely small, which allows to conclude that grid convergence has been reached.

The profiles of gas-dynamic parameters (velocity, density, temperature) are given in a normalized form on the basis of upstream and downstream Rankine-Hugoniot conditions. In this case, $\rho \rightarrow (\rho - \rho_1)/(\rho_2 - \rho_1)$; similarly for the temperature. For the velocity $u \rightarrow (u - u_2)/(u_1 - u_2)$.

Let the computational results for variant V2 be considered in detail. In Figs. 1 - 3 the profiles of gas-dynamic parameters at the shock-wave front are shown in comparison with the corresponding results obtained in [1] on the basis of the DSMC method. The curves, corresponding to the DSMC calculations, are superimposed on the QGDM data, so that the values of the mean density coincide at $x = 0$.

In Fig. 1 are the profiles of density and temperature of helium and xenon. In Fig.2a are the distributions of the mean density and temperature for the mixture. Like in the DSMC model, the mean temperature of the mixture is very close to that of helium; and the temperature of xenon overshoots its final value by $\sim 10\%$ and the mean mixture temperature is close to the helium temperature.

In Fig. 2b are presented the diffusion velocities u_{da} and u_{db} , reduced by the upstream flow velocity.

$$u_{da} = u_a - u, \quad u_{db} = u_b - u, \quad (21)$$

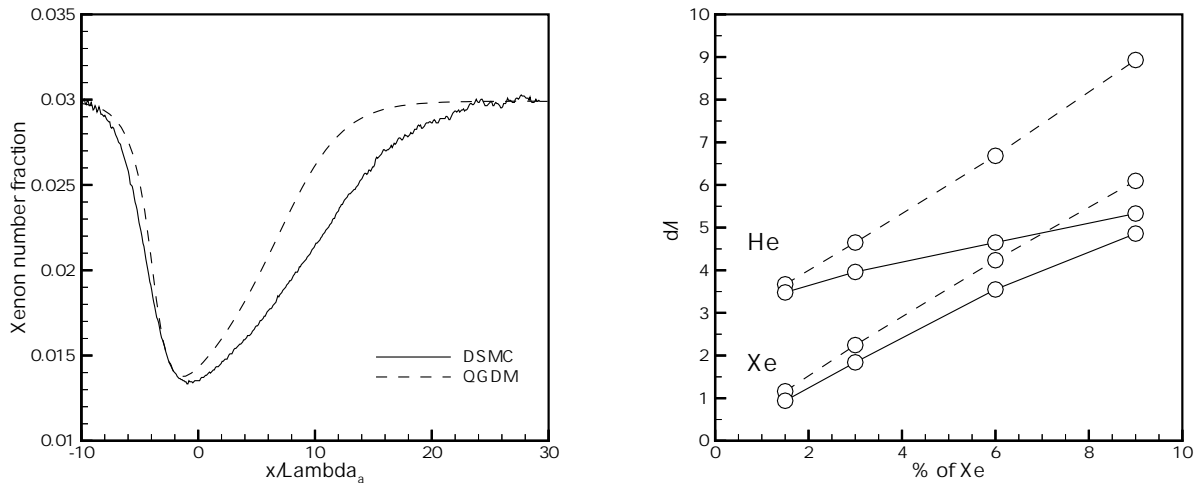


FIGURE 3. Diffusion velocities (a) and shock wave thickness (b) in a He-Xe mixture

where u is the mixture velocity that is defined according to (13).

In Fig. 3a the xenon concentration is presented. Within the shock wave, it falls to approximately half its initial value.

The curves demonstrate that the QGDM model reflects at least qualitatively the main features of the flow.

Variants V1, V3 and V4 correspond to the conditions of density measurements by Walenta [11]. The comparison of experimental results with those obtained by the present numerical work leads to the same conclusion.

On the basis of the calculations for variants V1 - V4 the shock-wave thicknesses δ_{He}/λ_{He} and δ_{Xe}/λ_{Xe} have been plotted in Fig.3b against the concentration of Xe in the upstream mixture and compared with the results of [11]. In this case, the shock-wave thickness is calculated as

$$\delta = \frac{\rho_2 - \rho_1}{\max(\partial\rho/\partial x)}. \quad (22)$$

The mean free path for each component is computed according to (17) for parameters of each gas component before the shock wave. The experimental data are plotted as a solid line; the authors' results as a dashed line. All the curves are represented in the form similar to [11]. For variant V1 (with the smallest Xe concentration), the experimental and computational results coincide practically. With increasing Xe concentration, the calculated shock wave thickness is larger than the experimental values. Nevertheless, the qualitative behavior is reproduced by the calculations. This is also consistent with the well-known fact that the relative shock wave thickness increases when the upstream Mach number decreases.

The shock wave thickness is a very sensitive characteristic feature of the problem, and its calculation based on moment equations for a single-component gas corresponds to the experimental data only in the case of small Mach numbers $Ma \leq 2$.

V ARGON – HELIUM DIFFUSION

As a second example of application of the QGDM equations, the problem of helium and argon mass diffusion was studied for conditions that correspond to a computation by the DSMC method [1]. Let two reservoirs, filled with the gases be located at a distance $L = 1\text{m}$. He is gas a in the right reservoir, and Ar is gas b in the left reservoir. The number densities in the reservoirs are kept constant and equal to $n = 2.8 \cdot 10^{20}\text{m}^{-3}$. The gases in the reservoirs are assumed to have the same temperature $T = 273\text{K}$ and the same velocity equal to zero.

Using these constants, the missing initial data can be obtained: helium density $\rho_a = nm_a = 1.862 \cdot 10^{-6}\text{kg/m}^3$; sound velocity $a_a = \sqrt{\gamma_a R_a T_a} = 971.9\text{m/s}$; mean free path computed by formula (17) $\lambda_a =$

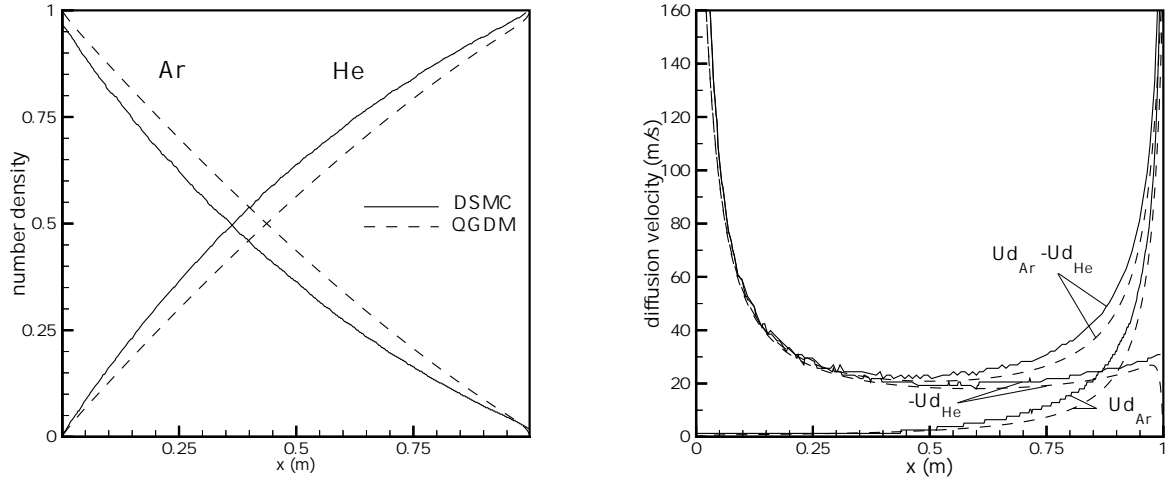


FIGURE 4. Number densities and diffusion velocities in the Ar - He diffusion problem.

$1.479 \cdot 10^{-2}$ m; argon density $\rho_b = nm_b = 1.856 \cdot 10^{-5}$ kg/m³; sound velocity $a_b = \sqrt{\gamma_b R_b T_b} = 307.81$ m/s; mean free path computed by formula (17) is $\lambda_b = 4.63 \cdot 10^{-3}$ m.

As in the previous section, computing was performed in dimensionless variables with all quantities normalized by the parameters of gas *a* - helium in the reservoir.

A one-dimensional plane flow described by equations (7) - (9) was considered. As boundary conditions the following non-dimensional relations were used:

at the left-hand boundary (1)

$$\rho_a = 1. - 10^{-10}, \quad \rho_b = 10^{-10}, \quad T_a = T_b = 1., \quad \frac{\partial u_a}{\partial x} = \frac{\partial u_b}{\partial x} = 0,$$

at the right-hand boundary (2)

$$\rho_b = 1. - 10^{-10}, \quad \rho_a = 10^{-10}, \quad T_a = T_b = 1., \quad \frac{\partial u_a}{\partial x} = \frac{\partial u_b}{\partial x} = 0.$$

That is, we assumed that in each reservoir a fraction $\sim 10^{-10}$ of the other gas exists. At initial time, the density of the components between the reservoirs is assumed to change linearly :

$$\rho_a(x) = \frac{\rho_a(x=L) - \rho_a(x=0)}{L}x + \rho_a(x=0),$$

$$\rho_b(x) = \frac{\rho_b(x=L) - \rho_b(x=0)}{L}x + \rho_b(x=0).$$

We used the same numerical algorithm as in the previous section when solving the QGDM equations. The problem was solved using a uniform space grid consisting of 339 points with spatial grid step $h = 0.2$, which corresponded to $0.2\lambda_a$ and $0.64\lambda_b$.

The number densities and diffusion velocities of both gases are plotted in Fig. 4 against the position between the reservoirs. In both figures the comparison with DSMC results [1] is given. Again the present results agree at least qualitatively with the reference results. The point of equal concentration point is shifted from the middle of the domain to the left, closer to the reservoir containing the heavier gas. The diffusion velocity of helium is larger than that of argon. The diffusion velocity of helium exhibits a minimum in the middle of the computational domain.

TABLE 1. Dimensional parameters of mixture components for variants V1–V4

| | V1 | | V2 | | V3 | | V4 | |
|----------------------------------|---------|-------|--------|-------|--------|-------|--------|-------|
| | He | Xe | He | Xe | He | Xe | He | Xe |
| $\rho(\text{kg/m}^3) \cdot 10^9$ | 5.15 | 2.57 | 5.16 | 2.22 | 4.91 | 10.3 | 4.57 | 14.8 |
| $p(\text{Pa})$ | 33.14 | 0.51 | 33.21 | 1.02 | 31.62 | 2.02 | 29.42 | 2.91 |
| $T(\text{K})$ | 310. | | | | | | | |
| $u(\text{m/s})$ | 3076.76 | | 2882.6 | | 2672.8 | | 2530.3 | |
| Ma | 2.97 | 17.01 | 2.78 | 15.93 | 2.58 | 14.78 | 2.44 | 13.99 |

VI CONCLUSION

The macroscopic system of the QGDM equations is constructed on the basis of the kinetic equation system in the relaxation approximation to describe the non-reacting-gas mixture flow. Contrary to some widely known models, the QGDM system consists of the equations for density, momentum and energy of each component, i.e. it is a two-fluid approximation, that makes it possible to describe in detail the behavior of each component.

The momentum and energy equations include exchange terms, that allow for the appropriate exchanges between the gas components. To calculate these terms the cross-collision frequencies must be estimated. The viscosity of the mixture must also be estimated. The QGDM model includes diffusion processes but does not require coefficients of thermo-, baro- and self- diffusion, which are included in the Navier-Stokes models, and the determination of which is a separate task.

The numerical algorithms developed on the basis of the QGDM model appear to be more stable than similar algorithms based on the conventional conservation equations.

Thus, the QGDM equations are worth being studied further for future other applications.

REFERENCES

1. Bird G.A. Molecular gas dynamics and the direct simulation of gas flows, Clarendon Press, Oxford, 1994.
2. Lapin Yu.V., Streleth M.H. Internal gas mixture flows. Moscow, Nauka, 1989. (in Russian)
3. Golovachev Yu.P. Numerical simulation of the viscous gas flow in a shock layer. Moscow, Nauka, "Fizmatlit", 1996. (in Russian)
4. Zhdanov V.M. Transport and relaxation processes in multicomponent plasma. Mir, Energoizdat, 1982. (in Russian)
5. Elizarova T.G., Chetverushkin B.N. Kinetic algorithms for calculating gasdynamic flows, *J.Comput. Mathem. and Mathem. Phys.* **25**, No5, 164 (1985).
6. Elizarova T.G., Graur I.A., Lengrand J.C., Chpoun A. Rarefied gas flow simulation based on quasigasdynamic equations. AIAA Journal. 1995. V.33. N 12. P.2316 – 2324.
7. Sheretov Yu.V., Quasi hydrodynamic equations as a model for viscous compressible heat conductive flows, in book: *Implementation of Functional Analysis in the Theory of Approaches*, Tver University, 127 (1997) (in Russian).
8. Elizarova T.G., Lengrand J.C., Graur I.A. Gradient expansions for distribution functions and derivation of moment equations, 21th Intern. Symp. on Rarefied Gas Dynamics, Marseille, France, July 26-30, 1998, Ed.R.Brun et al.. Cepadues, Toulouse, France, 1999, Vol.1, pp.119-126.
9. Chirokov I.A., Elizarova T.G., Lengrand J.C. Numerical study of shock wave structure based on quasigasdynamic equations with rotational nonequilibrium, 21th Intern. Symp. on Rarefied Gas Dynamics, Marseille, France, July 26-30, 1998, Ed.R.Brun et al.. Cepadues, Toulouse, France, 1999, Vol.1, pp.175-182.
10. Wu Y., Lee C.H. *Kinetic theory of shock tube problems for binary mixtures*, *J. Phys. of Fluids*.**14**, N 2, 313 (1971).
11. Gmurczyk A.S., Tarczyński M. and Walenta Z.A. Shock wave structure in the binary mixtures of gases with disparate molecular masses, Rarefied gas dynamics, Ed. by R. Campargue, CEA, Paris, v.1, 1979, pp. 333- 341.
12. Graur I.A, Elizarova T.G, Lengrand J.C. (1997) Quasigasdynamic equations with multiple translational temperatures, Laboratoire d'Aérodynamique du CNRS, Meudon (Fr), R 97-1.